College of Earth and Mineral Sciences

PENNSTATE

ANNUAL TECHNICAL REPORT

January 1992

OFFICE OF NAVAL RESEARCH

Contract NO. N00014-91-J-1528

POINT DEFECT EFFECTS ON HOT CORROSION OF ZIRCONIA-BASED COATINGS

R. Reidy and G. Simkovich

Depart of Materials Science and Engineering

The Pennsylvania State University

University Park, Pennsylvania 16802

PENN STATE
College of Earth and Mineral Sciences

Undergraduate Majors

Ceramic Science and Engineering, Fuel Science, Metals Science and Engineering, Polymer Science; Mineral Economics; Mining Engineering, Petroleum and Natural Gas Engineering; Earth Sciences, Geosciences; Geography; Meteorology.

Graduate Programs and Fields of Research

Ceramic Science and Engineering, Fuel Science, Metals Science and Engineering, Polymer Science; Mineral Economics; Mining Engineering, Mineral Processing, Petroleum and Natural Gas Engineering;
Geochemistry and Mineralogy, Geology, Geophysics; Geography; Meteorology.

Universitywide Interdisciplinary Graduate Programs Involving EMS Faculty and Students

Earth Sciences, Ecology, Environmental Pollution Control Engineering, Mineral Engineering Management, Solid State Science.

Associate Degree Programs

Metallurgical Engineering Technology (Shenango Valley Campus).

Interdisciplinary Research Groups Centered in the College

C. Drew Stahl Center for Advanced Oil Recovery, Center for Advanced Materials, Coal Research Section, Earth System Science Center, Mining and Mineral Resources Research Institute, Ore Deposits Research Group.

Analytical and Characterization Laboratories (Mineral Constitution Laboratories)

Services available include: classical chemical analysis of metals and silicate and carbonate rocks; X-ray diffraction and fluorescence; electron microscopy and diffraction; electron microprobe analysis; atomic absorption analysis; spectrochemical analysis; surface analysis by secondary ion mass spectrometry (SIMS); and scanning electron microscopy (SEM).

U.Ed. 87-1027
Produced by the Penn State Department of Publications

SECURITY CLASSIFICATION OF THIS PAGE

REPORT DOCUMENTATION PAGE

1a. REPORT SECURITY CLASSIFICATION	1b. RESTRICTIVE MARKINGS
2a. SECURITY CLASSIFICATION AUTHORITY	3. DISTRIBUTION/AVAILABILITY OF REPORT
2b. DECLASSIFICATION/DOWNGRADING SCHEDULE	
4. PERFORMING ORGANIZATION REPORT NUMBER(S) Metallurgy Program, 209 Steidle Bldg.	5. MONITORING ORGANIZATION REPORT NUMBER(S)
6a. NAME OF PERFORMING ORGANIZATION Metallurgy Program 6b. OFFICE SYMBOL (If applicable)	7a. NAME OF MONITORING ORGANIZATION Metallurgy Branch
6c. ADDRESS (City, State and ZIP Code) 209 Steidle Bldg. The Pennsylvania State University University Park, PA 16802	7b. ADDRESS (City, State and ZIP Code) Office of Naval Research Arlington, VA 22217
8a. NAME OF FUNDING/SPONSORING ORGANIZATION Metallurgy Branch 8b. OFFICE SYMBOL (If applicable)	9. PROCUREMENT INSTRUMENT IDENTIFICATION NUMBER N000-14-91-J-1528 (contract number)
8c. ADDRESS (City, State and ZIP Code) Office of Naval Research Arlington, VA 22217	10. SOURCE OF FUNDING NOS PROGRAM ELEMENT NO. / PROJECT NO / TASK NO / WORK UNIT NO.

11. TITLE (Include Security Classification)
Point Defect Effects on Hot Corrosion of Zirconia-based Coatings

12. PERSONAL AUTHOR(S)
R. Reidy and G. Simkovich

13a. TYPE OF REPORT	13b. TIME COVERED	14. DATE OF REPORT (Yr., Mo., Day)	15. PAGE COUNT
Annual Technical Report	FROM 1-91 TO 1-92	1-16-92	

16. SUPPLEMENTARY NOTATION

17. COSATI CODES			18. SUBJECT TERMS (Continue on reverse if necessary and identify by block number)
FIELD	GROUP	SUB GR	

19. ABSTRACT (Continue on reverse if necessary and identify by block number)

Thermal barrier coatings are vulnerable to certain types of hot corrosion: sulfidation and vanadic attack. Stabilized zirconia, an often used thermal barrier coating, is degraded by dissolution of the stabilizing component (e.g. Y_2O_3). To obtain the dissolution of the stabilizing components, mass transport in the coating must occur. The presence of point defects in a crystalline solid greatly affect the transport properties in that solid. The nature and concentration of these defects can be altered which, in turn, can impart large changes in the transport properties of a material (eg. ionic conductivity and diffusion). In this study, we are determining the defect structures of yttria and ceria-stabilized zirconium oxides. Using electrical conductivity measurements, the activation energies of yttria-stabilized zirconia have been examined as a function of grain size and composition.
(see back)

20. DISTRIBUTION/AVAILABILITY OF ABSTRACT UNCLASSIFIED/UNLIMITED ☐ SAME AS RPT ☐ DTIC USERS ☐	21. ABSTRACT SECURITY CLASSIFICATION
22a. NAME OF RESPONSIBLE INDIVIDUAL	22b. TELEPHONE NUMBER (Include Area Code) / 22c. OFFICE SYMBOL

DD FORM 1473, 83 APR EDITION OF 1 JAN 73 IS OBSOLETE

SECURITY CLASSIFICATION OF THIS PAGE

Using nano-crystalline powders, activation energies increased as a function of grain size. Conductivity measurements on ceria-stabilized zirconia have been conducted as a function of temperature, composition, and oxygen activity. At low oxygen activities, ZrO_2-CeO_2 samples evidenced n-type behavior. At more moderate oxygen partial pressures, oxygen vacancies were the dominant charge carriers.

ABSTRACT

Thermal barrier coatings are vulnerable to certain types of hot corrosion: sulfidation and vanadic attack. Stabilized zirconia, an often used thermal barrier coating, is degraded by dissolution of the stabilizing component (e.g. Y_2O_3). To obtain the dissolution of the stabilizing components, mass transport in the coating must occur. The presence of point defects in a crystalline solid greatly affect the transport properties in that solid. The nature and concentration of these defects can be altered which, in turn, can impart large changes in the transport properties of a material (eg. ionic conductivity and diffusion). In this study, we are determining the defect structures of yttria and ceria-stabilized zirconium oxides. Using electrical conductivity measurements, the activation energies of yttria-stabilized zirconia have been examined as a function of grain size and composition. Using nano-crystalline powders, activation energies increased as a function of grain size. Conductivity measurements on ceria-stabilized zirconia have been conducted as a function of temperature, composition, and oxygen activity. At low oxygen activities, ZrO_2-CeO_2 samples evidenced n-type behavior. At more moderate oxygen partial pressures, oxygen vacancies were the dominant charge carriers.

INTRODUCTION

Due to the severity of their operating environments, marine turbines are subject to a variety of corrosive mechanisms. One of the most formidable forms of attack is hot corrosion, a chemical interaction leading to a breakdown of a protective oxide scale.(1) There are two dominant types of hot corrosion: sulfidation and vanadium attack.

In sulfidation, NaCl reacts with sulfur found in the fuel to form Na_2SO_4. The sodium sulfate reacts with the protective oxide scale resulting in scale failure.(1,2) A large body of work details the roles of Na_2SO_4 and NaCl in the destruction of the oxide scale.(1-8)

Vanadium enters the turbine as a fuel impurity in organic and inorganic forms. These compounds react with oxygen to form oxides (VO, VO_2, VO_3, and V_2O_5) and hydroxides ($V_2O_7H_4$, $VO(OH)_3$, and $VO_2(OH)_2$).(9) These gases either condense onto the turbine blades and react with sodium compounds to form sodium vanadates as in equations 1-3),

$$2VO(OH)_3(g) = V_2O_5(l) + 3H_2O(g) \quad 1)$$

$$V_2O_5(g) = V_2O_5(l) \quad 2)$$

$$V_2O_5(l) + Na_2O(l) = 2NaVO_3(l) \quad 3)$$

or react with sodium compounds in the gas phase forming sodium vanadates which condense onto the turbine blades as in equation 4).

$$VO(OH)_3(g) + NaOH(g) = NaVO_3(l) + 2H_2O(g) \quad 4)$$

In addition to Na_2SO_4, Luthra and Spacil found both V_2O_5 and $NaVO_3$ in the condensate; therefore, it is difficult to determine which compound is more destructive to the oxide.(9) Further, one can not ignore the effects of Na_2SO_4 in a separate or combined attack on the oxide scale.

The mechanisms by which the sulfur or vanadium compounds disrupt protective oxide scales of nickel-based superalloys in marine turbine hot zones are detailed in several literature surveys.(1,7,10) Bornstein and DeCrescente (2) and Jones (8) describe a general mechanism referred to as the salt fluxing or acid-base reaction model. In sulfidation, Bornstein explains that the oxide scales are insoluble in stoichiometric sodium sulfate, but due to the reaction,

$$\underset{\text{(molten salt)}}{Na_2SO_4(l)} = \underset{\text{(base)}}{Na_2O} + \underset{\text{(acid)}}{SO_3} \qquad 5)$$

the oxide may dissolve in the base as an anion or in the acid as a cation.(1) From the Lux-Flood theory (11), the activities of the acidic and basic components in the molten salt are fixed by the dissociation constant of the reversible reaction 5).(8) In vanadium attack, a similar dissolution mechanism utilizes the Lewis definition of acids (electron acceptors) and bases (electron donors). Jones describes the ability of vanadium pentoxide to behave as a Lewis acid and react with a protective oxide.(8)

$$\underset{\text{(base)}}{Y_2O_3(s)} + \underset{\text{(acid)}}{V_2O_5(l)} = \underset{\text{(salt)}}{2YVO_4(l)} \qquad 6)$$

This dissolution mechanism involves the transport of electrons from the stabilizing component to the corrosive V_2O_5. A greater understanding of this transport phenomenon could yield the ability to retard or halt this dissolution.

Defect Chemistry

Rarely in nature does one find a perfect crystal. Instead, a number of disruptions occur in the periodic array of atoms. There are four general types of structural imperfections: point defects, line defects, plane defects, and

volume defects.(12) In crystalline solids, the nature and concentration of point defects greatly affect transport properties.

The type and concentration of point defects in an oxide is often dependent on the temperature, pressure, and chemical potentials of the oxide components.(13) Atomic defects (vacancies, interstitials, impurities, or misplaced atoms) affect solid state diffusion and non-stoichiometry of compounds. Changes in these properties, in turn, alter reaction rates, ionic conductivities, and sintering rates. Electronic defects (electrons and electron holes) determine electrical conductivities as well as other properties.(14,15) Therefore, a detailed understanding of the point defect behavior of a compound would provide great insight or even allow one to predict the transport phenomena in that material. Additionally, one may alter the transport properties of a compound by changing the nature or concentration of the point defects within it.

The effects of point defects on hydrometallurgical processes, such as flotation and dissolution, have been the subject of many studies.(16) In lead sulfide (PbS) which shows p-type conduction at high S_2 partial pressures and n-type at low S_2 partial pressures, additions of Ag_2S impart more p-type behavior while Bi_2S_3 doping creates a larger n-type contribution.(17) When the reaction rate is controlled by the interfacial reaction, Simkovich and Wagner found that the dissolution rates in nitric acid of PbS containing Ag_2S are greater than both pure PbS and Bi_2S_3-doped PbS.(16) Similar effects of dopant-induced changes in dissolution rates in NiO (17) and ZnO (18) have been documented. Some alterations in the defect structure of a base material which result in changes in dissolution behavior are an increased concentration of electron holes in Li_2O-doped NiO (19) and an increase in zinc interstitials in Li_2O-doped ZnO (20). Simkovich and Wagner detail other systems and the mechanisms by which changes in defect concentration directly affect dissolution rates.(21-26)

Thermal Barrier Coatings

In recent years, efforts have been made to apply protective ceramic coatings to turbine blades to improve resistance to hot corrosion as well as to increase engine operating temperatures.(27-29) These higher operating temperatures are attained because these coatings have high melting points and low thermal conductivities, thus protecting the more temperature sensitive alloy beneath. These materials are referred to as thermal barrier coatings.

With additions of various stabilizers, zirconia has been used as a thermal barrier coating. Due to a relatively high coefficient of thermal expansion (as compared to other ceramics), ZrO_2 minimizes thermal expansion differences between metal substrate and coating. However, the primary reason for considering stabilized ZrO_2 as a thermal barrier coating is its resistance to many forms of corrosion.

Pure zirconium oxide is a polymorphic compound. Three different stable forms of zirconia exist: cubic (fluorite structure, 2370 - 2680°C), tetragonal (1170 - 2370°C), and monoclinic (below 1170°C).(30) The phase transition from tetragonal to monoclinic has caused considerable concern. Early studies have determined that the transformation is martensitic (31) and does not occur at a fixed temperature, but over a temperature range, and involves a large (about 9%) volume expansion. This volume increase causes cracking in the ZrO_2 when cooled below the transition; therefore, traditional cooling methods to below 1170°C can result in crumbling of the zirconia.

The addition of CaO, MgO, Y_2O_3, and CeO_2 to zirconia lowers the transition temperatures of both solid state phase transformations.(30) Stubican and Hellmann (32) have reviewed the binary oxide phase diagrams and have shown a partially stabilized form (a mixture of cubic and tetragonal or monoclinic phases) and a fully stabilized zirconia (cubic phase). Both the cubic and mixed phases are stable at room temperature.

Wagner demonstrated that stabilized zirconia contains oxygen ion vacancies.(33) In calcia-stabilized zirconia, Hund (34) discovered that calcium

and zirconium ions are distributed statistically in the cation sites while an oxygen vacancy concentration equal to the calcium dopant concentration provides electroneutrality. Using x-ray diffraction methods, Tien and Subbarao have determined similar defect behavior in other stabilized zirconias.(35) Other investigators have concluded that the defect structure and concentration are fixed by dopant content.(36-40) Alcock has found that the electronic defect structure of stabilized zirconia is affected by changes in atmosphere and temperature.(41)

The primary thrust of this work is to determine the effect of point defects on the mechanisms and transport properties involved in the hot corrosion of zirconia coatings. It is prudent to briefly review the recent efforts to study these mechanisms by other methods.(5,42,43) The sulfidation and vanadium attack studies by Jones and Williams (44,45) demonstrated that ZrO_2 is substantially more resistant to hot corrosion than the dopants, Y_2O_3, CeO_2, and HfO_2. In other work, Jones discusses the degradation of the coating with respect to the acid-base reaction model.(5) The V_2O_5 reacts with the Y_2O_3 in the zirconia and forms a yttrium vanadate (equation 5)). The removal of yttria destabilizes the zirconia allowing the more voluminous monoclinic phase to form and leading to surface cracking of the coating. As the protective scale is thermally cycled, the cracks propagate and extend into the coating causing spallation. This mechanism has been put forth by a number of other investigators.(46-48)

EXPERIMENTAL

Electrical and Ionic Conductivity

The electrical conductivity will be measured by a digital bridge using a two-point probe or a four-wire technique. The conductivity measurements will be taken at a number of temperatures (700-1100°C) and oxygen partial pressures. In addition, an Arrhenius plot of conductivity and temperature can

estimate the activation energy of conduction.(7) By definition, conductivity is the product of the charge, the concentration of charge carriers, and the mobilities of those carriers. In an electrical conductivity measurement, the carriers can be either electronic or ionic.

Materials

In order to accurately describe the point defect structure of a material, the effects of macroscopic flaws such as pores and cracks should be reduced or, if possible, eliminated. As stated earlier, most commercial zirconia powders that were available did not fully densify during sintering. After a number of attempts, only one commercial powder had the necessary purity and could be fully densified (achieve densities 95% of theoretical values). Samples fabricated from other powders gave unreliable results. In order to control densities, composition, and purity, powders were synthesized by coprecipitation reactions. Using a protocol adapted from the work by Ciftcioglu and Mayo (49), nano-crystalline powders were prepared. By controlling sintering temperatures and times, one can fix sample grain size. A coprecipitation procedure for CeO_2-ZrO_2 by Duh et al. (50) may also be adapted to yield nano-crystalline powders.

RESULTS

Electrical Measurements

In the past year, efforts were concentrated on three materials: Y_2O_3-ZrO_2, CeO_2-ZrO_2, and nano-crystalline Y_2O_3-ZrO_2. Electrical conductivity measurements as a function of oxygen activity and temperature were performed on large grained yttria-stabilized zirconia. Plots of conductivity versus 1/T for these samples evidenced linear behavior indicating single activation energies. This suggested only a single conduction mechanism.

Electrical conductivity measurements for 3 mole percent yttria-stabilized

zirconia provided some interesting results. For large-grained samples, conductivity behaved in accordance with the literature values (the activation energies were approximately 1 eV)(30); however, nanocrystalline powders produced samples with activation energies which were lower than expected. These nano-powders successfully sintered to high densities at temperatures well below commercial powders (Tosoh powder has a grain size of 300 nm). In addition, samples were obtained from Drs. Mayo (Penn State) and Ciftcioglu (University of New Mexico) which were sintered at 1100°C to form very small grains (60 nm). (These materials are designated as sample UNM.) As the sintering temperature increases, the grain size increases. Table I lists the activation energies of a commercial powder (Tosoh) and a nano-powder sintered at three different temperatures.

TABLE I

Composition	***Activation Energy (eV)***
3m/o Y_2O_3-ZrO_2 (Tosoh) sintered at 1600°C	.989 ± .093
3m/o Y_2O_3-ZrO_2 (nanocrystalline) sintered at 1350°C	.827 ± .048
3m/o Y_2O_3-ZrO_2 (nanocrystalline) sintered at 1300°C	.838 ± .052
3m/o Y_2O_3-ZrO_2 (nanocrystalline) sintered at 1100°C (UNM)	.720 ± .019

The grain sizes for the samples sintered at 1300 and 1350°C have not yet been measured, but are certainly larger than the 1100°C material. It seems evident that large- and nano-grained yttria-stabilized zirconias have different conduction mechanisms. Impedance spectroscopy measurements have been undertaken to determine the influence of grain boundary conduction, but the results are

incomplete at present.

In two ceria-stabilized samples, 12 and 15 mole percent CeO_2, the temperature-conductivity behavior was quite unusual. The conductivity curves during heating and cooling do not match (Fig.1 and 2). This behavior was reproducible over three cycles. This phenomenon may suggest ordering and disordering of the oxygen vacancies. High temperature x-ray measurements are currently underway to explain these results. In contrast, the 20m/o CeO_2-ZrO_2 (Fig.3) showed a single slope during heating and cooling. As a function of oxygen activity, three distinct conduction regions were found: at low P_{O2}'s, n-type; at medium P_{O2}'s, anti-Frenkel, and at high P_{O2}'s, an as yet undetermined conduction mechanism (Fig.4). Impedance spectroscopy data showed some evidence of grain boundary conduction at low oxygen partial pressures while results in air indicated that bulk conduction dominated.

CONCLUSIONS

The aim of this research is to characterize the conduction mechanisms and defect behavior of yttria- and ceria-stabilized zirconia. Using temperature-conductivity measurements supported with impedance spectroscopy, the activation energies of large-grained and nano-grained Y_2O_3-ZrO_2 samples have been found to differ greatly. It is believed that bulk conduction dominates in the larger-grained system while grain boundary conduction provides the primary conduction mechanism for the nano-powder materials.

In the 12 and 15 m/o ceria-stabilized systems, two distinct conductivity curves occur during thermal cycling. This difference between heating and cooling behavior may be the result of an ordering and disordering of oxygen vacancies. In the 20 mole percent CeO_2-ZrO_2 samples, thermal cycling produced a single-sloped curve. High temperature x-ray diffraction should provide a reasonable explanation for this behavior. Conductivity-oxygen activity measurements detailed three regions in the ceria-zirconia system: n-type

semiconductor behavior at low oxygen partial pressures, anti-Frenkel disorder at more moderate P_{O2}'s, and an unknown defect near ambient conditions. Impedance spectroscopy experiments conducted in air indicate that there is a grain boundary contribution to the electrical conductivity.

REFERENCES

1. Bornstein, N. S., Literature Review of Inhibition of Vanadate Attack, ONR N00014-88-M-0013, June 1988

2. Bornstein, N. S. and M.A. DeCrescente, Corrosion, 26, 7, 209-14, July 1988

3. Luthra, K. and D. Shores, A Study of the Mechanism of Hot Corrosion in Environments Containing NaCl, NRL Contract N000173-77-C-0253, Fifth Quarterly Progress Report, November 1978

4. Luthra, K. and D. Shores, A Study of the Mechanism of Hot Corrosion in Environments Containing NaCl, NRL Contract N000173-77-C-0253, Sixth Quarterly Progress Report, February 1979

5. Luthra, K. and D. Shores, A Study of the Mechanism of Hot Corrosion in Environments Containing NaCl, NRL Contract N000173-77-C-0253, Sixth Quarterly Progress Report, May 1979

6. Jones, R. L. and S. Gadomski, J. Electrochem. Soc., 124, 10, 1641-1648, 1977

7. Shores, D., D. McKee, and T. Kerr, Sodium Chloride Induced Hot Corrosion: Literature Survey and Preliminary Experiments, Contract 7A003-CIP105 (EPNHT05), April 1976

8. Jones, R. L., Low Quality Fuel Problems With Advanced Materials, NRL Report 6252, August 1988

9. Luthra, K. and H. Spacil, J. Electrochem. Soc., 129, 3, 649-656, 1982

10. Fitzer, E. and J. Schwab, Corrosion, 12, 49-54, 1956

11. Flood, H. and T. Forland, Acta Chem. Scand., 1, 592, 1947

12. Kingery, W., H. Bowen, and D. Uhlmann, Introduction to Ceramics, 2nd edition, Wiley, New York, 1976, p.125

13. Su, M. Y., Point Defect Structure of Chromium Sesquioxide, PhD thesis, Penn State Univ., 1987, p.4-6

14. Kroger, F. A., Chemistry of Imperfect Crystals, Wiley, New York, 1964, p.194

15. Simkovich, G. and F. F. Aplan, "The Influence of Solid State Imperfections in Mineral and Metal Processing", Metallurgical Processes for the Year 2000 and Beyond, ed. by Sohn, H. Y. and E. S. Geskin, The Mineral, Metals & Materials Society, 1988

16. Simkovich, G. and J. B. Wagner, Jr., J. Electrochem. Soc., 110, 513-516, 1963

17. Nii, K., Corr. Sci., 10, 571-583, 1970

18. Jones, C. F., R. L. Segall, R. St. C. Smart, and P. S. Turner, J. Chem. Soc., Faraday Trans. I., 73, 1710-1720 , 1978

19. Jones, C. F., R. L. Segall, R. St. C. Smart, and P. S. Turner, J. Chem. Soc., Faraday Trans. I., 74, 1615-1624, 1978

20. Jones, C. F., R. L. Segall, R. St. C. Smart, and P. S. Turner, J. Chem. Soc., Faraday Trans. I., 74, 1624-1633 , 1978

21. Illis, A., G. Nowlan, and J. Koehler, CIM Bulletin, 63, 352-361, 1970

22. Lussiez, P. K. Osseo-Asare, and G. Simkovich, Met. Trans., 12B, 651-657, 1981

23. Rogers, G., G. Simkovich, and K. Osseo-Asare, Hydrometallurgy, 10, 313-328, 1983

24. Wan, R. Y., J. D. Miller, and G. Simkovich, "Enhanced Ferric Sulfate Leaching of Cu from $CuFeS_2$ and Carbon Particle Aggregates", Inter. Conf. on Recent Adv. in Min. Sci. and Tech., MINITEK 50, 1984

25. Wagner, C., J. Phys. Chem. Solids, 33, 1051-1059, 1972

26. Beckmann, J. D., A. Birchenall, and G. Simkovich, "Electrical Conductivity of Dispersed Phase Systems", First Inter. Conf. on Transport of Non-Stoichiometric Compounds, ed. by J. Nowotny, Elsevier Sci., New York, 1982, p.8-28

27. Liebert, C., R. Jacobs, S. Stecura, and C. Morse, "Durability of Zirconia Thermal Barrier Coatings on Air Cooled Turbine Blades in Cyclic Jet Engine Operation", NASA TM X-3410, Sept. 1976

28. Sevcik, W. and B. Stoner, "Analytical Study of Thermal Barrier Coated First-stage Blades In a JT9D Engine", NASA CR-135360, Jan. 1977

29. Carlson, N. and B. Stoner, "Study of Thermal Barrier Coatings on High Temperature Industrial Gas Turbine Engines", NASA CR-135147, Feb. 1978

30. Subbarao, E. C., "Zirconia an Overview", Science and Technology of Zirconia, Advances in Ceramics Vol.3, ed, by Heuer, A. H. and L. W. Hobbs, Amer. Cer. Soc., 1981, p. 1-24

31. Wolten, G. W., J. Amer. Cer. Soc., 46, 9, 418-22, 1963

32. Stubican, V. S. and J. R. Hellmann, "Phase Equilibria in Some Zirconia Systems", Science and Technology of Zirconia, Advances in Ceramics Vol.3, ed, by Heuer, A. H. and L. W. Hobbs, Amer. Cer. Soc., 1981, p.25-36

33. Wagner, C., Naturwissenschaften, 31, 265-68, 1943

34. Hund, F., Z. Phys. Chem., 199, 142-51, 1952

35. Tien, T. Y., and E. C. Subbarao, J. Chem. Phys., 39, 4, 1041-47, 1963

36. Etsell, T. H.,and S. N. Flengas, Chem. Rev., 70, 339--76, 1970

37. Takahashi, T., Physics of Electrolytes Vol. 2, ed. by J. Hladik, Academic Press, New York, 1972, p.989-1051

38. Worrell, W. E., Solid Electrolytes, ed. by S. Geller, Springer-Verlag, Berlin, 1977, p.143-168

39. Dell, R. M., and A. Hooper, Solid Electrolytes, ed. by P. Hagenmuller and W. Van Gool , Academic Press, New York, 1978, p.291-312

40. Choudhary, C. B., H. S. Maiti, and E. C. Subbarao, Solid Electrolytes and their Applications, ed. by E. C. Subbarao, Plenum Press, New York, 1980, p.1-80

41. Alcock, C. B., "Transport of Ions and Electrons in Ceramic Oxides", Electromotive Force Measurements in High-temperature Systems, ed. by Alcock, C. B., Institution of Mining and Metallurgy, 1968

42. Patton, J. S. and R. L. Clarke, "Hot Corrosion Resistance of Yttria-Stabilized Zirconia Coatings", 1989 Tri-Service Corrosion Conference, 1989

43. Nagelberg, A. S., J. Electrochem. Soc., 132, 2502, 1985

44. Jones, R. L., and C. E. Williams, J. Electrochem. Soc., 132, 1498, 1985

45. Jones, R. L., and C. E. Williams, J. Electrochem. Soc., 133, 227, 1986

46. Singhal, S. and R. J. Bratton, "Stability of a $ZrO_2(Y_2O_3)$ Thermal Barrier Coating in Turbine Fuel with Contaminant", J. Eng. for Power, 102, 4, 770-775, 1980

47. Palko, J., K. Luthra, and D. McKee, "Evaluation of performance of Thermal Barrier Coatings Under Simulated Industrial/Utility Gas Turbine Conditions", Final Report, General Electric Co., 1978

48. Zaplatynsky, I., "Reactions of Yttria-Stabilized Zirconia with Oxides and Sulfates of Various Elements", DOE/NASA/2593-78/1, NASA TM-78942, 1978

49. Ciftcioglu, M. and M.J. Mayo, Material Research Society Symposium Proceeding, Vol.196, ed. by M.J. Mayo, M. Kobayashi, and J. Wadsworth, Pittsurgh, 1990, p. 77

50. Duh, J.G., H.T. Dai, and W.Y. Hsu, J. Mat. Sci., 23, 2786, 1988

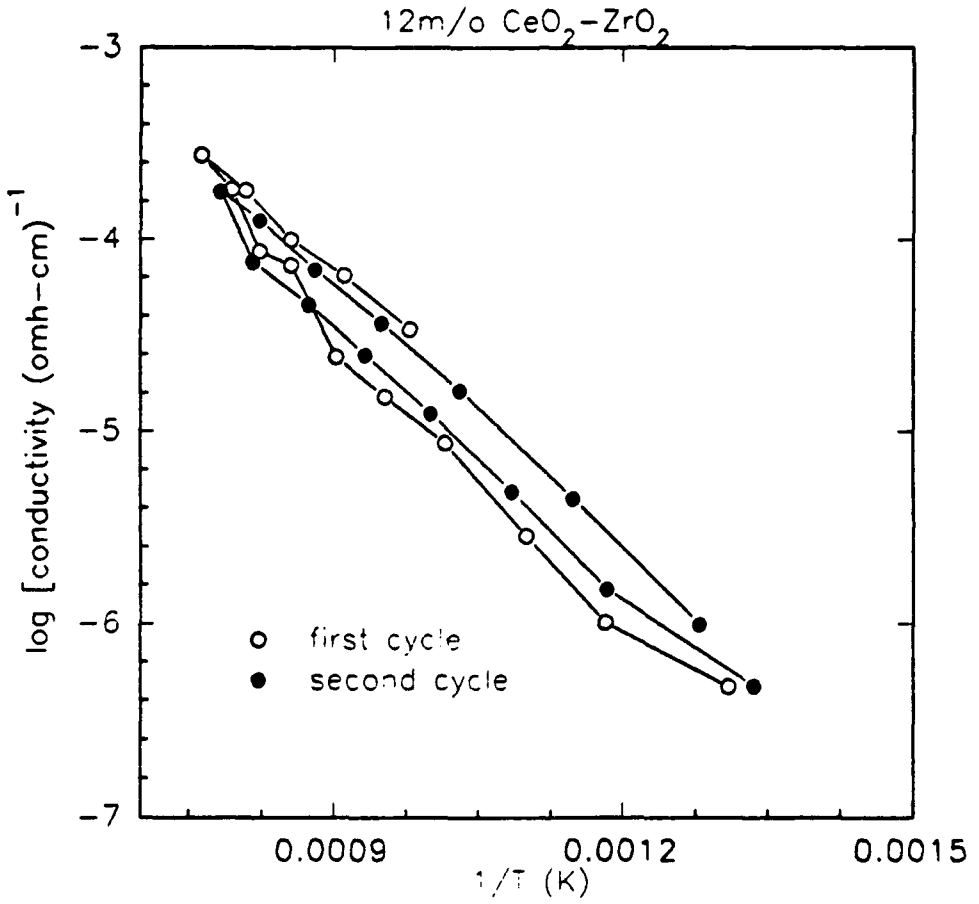

Figure 1 Thermal cycling behavior for 12m/o CeO_2-ZrO_2

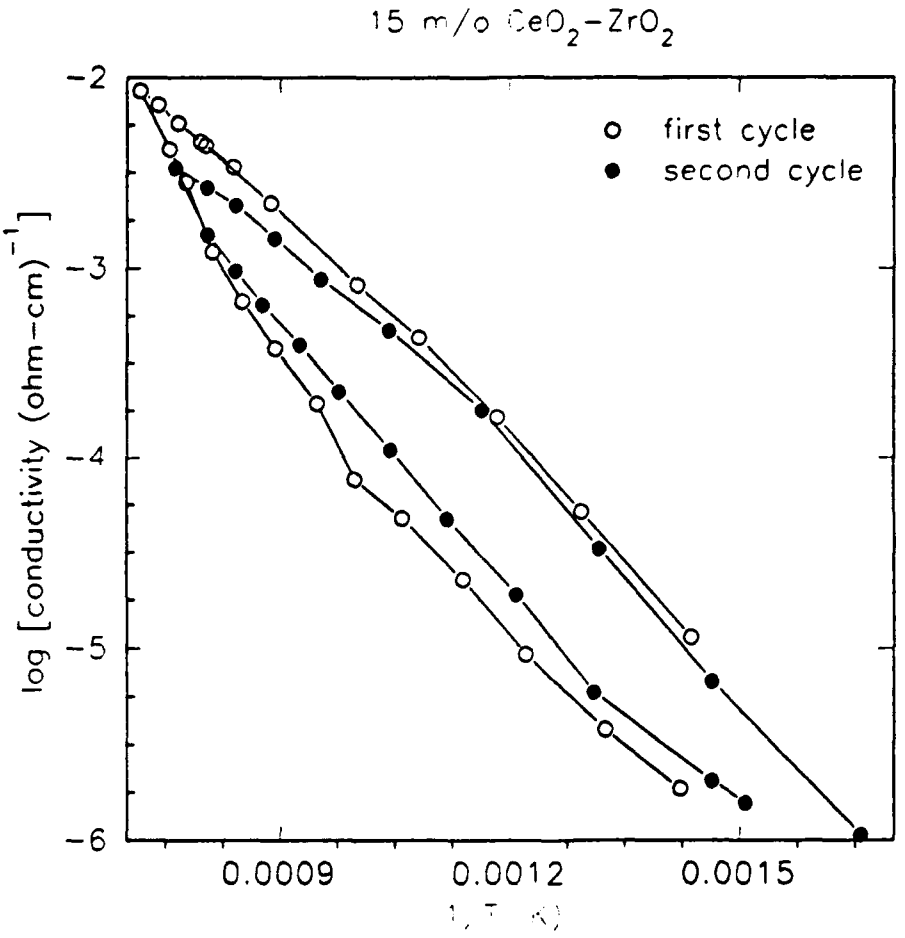

Figure 2 Thermal cycling behavior for 15m/o CeO_2-ZrO_2

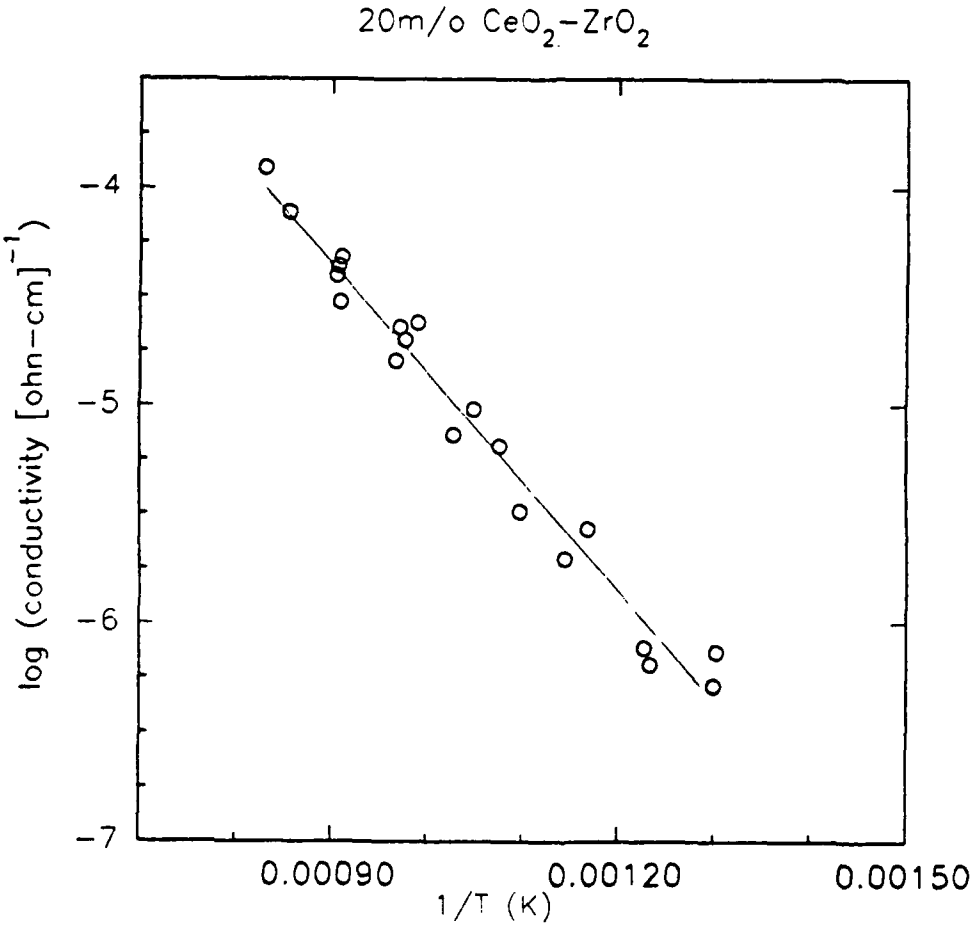

Figure 3 Thermal cycling behavior for 20m/o CeO_2-ZrO_2

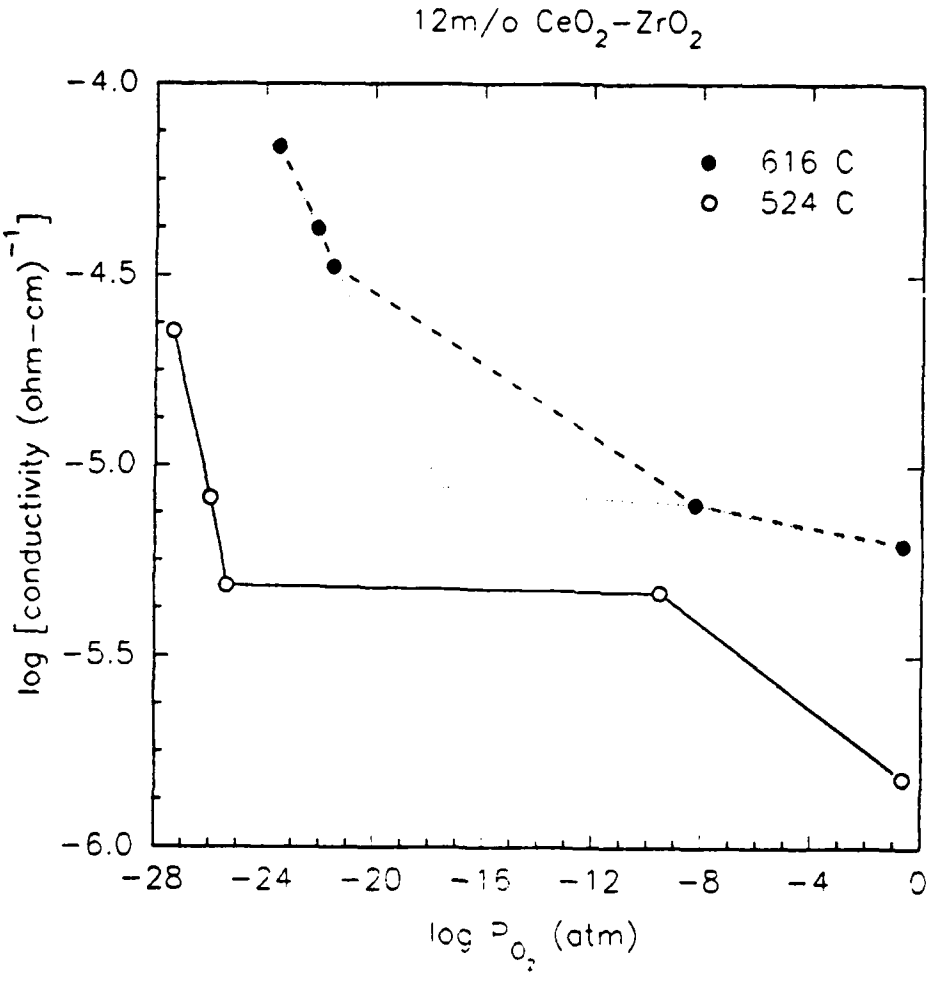

Figure 4 Electrical conductivity versus oxygen partial pressure for 12m/o CeO_2-ZrO_2